Pig Heart CoA Transferase Exists as Two Oligomeric Forms Separated by a Large Kinetic Barrier†

Jean-Christophe Rochet,[‡,§] Edward R. Brownie,[‡] Kim Oikawa,[‡,||] Leslie D. Hicks,[‡,||] Marie E. Fraser,[‡,⊥,#] Michael N. G. James,[‡,⊥] Cyril M. Kay,[‡,||] William A. Bridger,[▽] and William T. Wolodko*[,‡]

Department of Biochemistry, University of Alberta, Edmonton, Alberta, Canada T6G 2H7, Protein Engineering Network of Centres of Excellence, University of Alberta, Edmonton, Alberta, Canada T6G 2H7, Medical Research Council of Canada Group in Protein Structure and Function, University of Alberta, Edmonton, Alberta, Canada T6G 2H7, and Office of the VP Research, University of Western Ontario, London, Ontario, Canada N6A 5B8

Received February 10, 2000; Revised Manuscript Received May 22, 2000

ABSTRACT: Pig heart CoA transferase (EC 2.8.3.5) has been shown previously to adopt a homodimeric structure, in which each subunit has a molecular weight of 52 197 and consists of N- and C-domains linked by a hydrophilic linker or "hinge". Here we identify and characterize a second oligomeric form constituent in purified enzyme preparations, albeit at low concentrations. Both species catalyze the transfer of CoA with similar values for k_{cat} and K_M. This second form sediments more rapidly than the homodimer under the conditions of conventional sedimentation velocity and active enzyme centrifugation. Apparent molecular weight values determined by sedimentation equilibrium and gel filtration chromatography are 4-fold greater than the subunit molecular weight, confirming that this form is a homotetramer. The subunits of both oligomeric forms are indistinguishable with respect to molecular mass, far-UV CD, intrinsic tryptophan fluorescence, and equilibrium unfolding. Dissociation of the homotetramer to the homodimer occurs very slowly in benign solutions containing high salt concentrations (0.25−2.0 M KCl). The homotetramer is fully converted to homodimer during refolding from denaturant at low protein concentrations. Disruption of the hydrophilic linker between the N- and C-domains by mutagenesis or mild proteolysis causes a decrease in the relative amount of the larger conformer. The homotetramer is stabilized by interactions involving the helical hinge region, and a substantial kinetic barrier hinders interconversion of the two oligomeric species under nondenaturing conditions.

The coenzyme A (CoA)[1] transferases catalyze the transfer of CoA from an acyl-CoA donor to a carboxylate acceptor. These enzymes play a key role in prokaryotic and eukaryotic metabolism, as they enable the activation of various carbon compounds for subsequent oxidation. In mammals, the mitochondrial enzyme succinyl-CoA:3-ketoacid CoA transferase (EC 2.8.3.5) catalyzes the transfer of CoA from succinyl-CoA to acetoacetate, an essential step in the metabolism of ketone bodies (*1*, *2*).

From the results of early studies of CoA transferases from pig heart (*3*−*5*), sheep kidney (*6*), and rat brain (*7*), it was proposed that the mammalian enzyme exists as a homodimer. Each subunit of the "mature" enzyme from pig heart consists of 481 amino acid residues and has a molecular weight of 52 197 (*8*). A hydrophilicity plot suggests a structure of two relatively hydrophobic regions, connected by a sequence of hydrophilic residues referred to as a "linker" or "hinge" segment (*8*). Given the distribution of acidic and basic residues in this segment, the hinge likely adopts a helix−turn−helix motif with positive and negative charges clustering on opposite faces of the α-helices (*8*). Molecular weights determined by gel filtration chromatography, sedimentation equilibrium, nondenaturing PAGE, or cross-linking and SDS−PAGE ranged from 7.8×10^4 to 1.13×10^5, equivalent to 1.5−2.2 times the subunit molecular weight (*3*−*8*). In addition, the free enzyme was converted stoichiometrically to ECoA upon incubation with 2 molar equiv of acyl-CoA substrate, as determined from the maximal extent of inactivation by 5,5′-dithiobis(2-nitrobenzoic) acid (DTNB) (*9*), by acetohydroxamic acid (AHA) (*10*, *11*), or by methylmercaptopropionate (MMP) (*12*). Thus, 2 mol of active sites was titrated for each mole of CoA transferase, consistent with a homodimeric structure.

† This work was funded by grants from the Medical Research Council of Canada (MRC Grant MT-2805) and the Protein Engineering Network Centres of Excellence. J.-C.R. was supported by studentships from the MRC and the Alberta Heritage Foundation for Medical Research.

* To whom correspondence should be addressed. Telephone: (780) 492-2419; FAX: (780) 492-0886; E-mail: wtwt@obi-wab.biochem.ualberta.ca.

‡ Department of Biochemistry, University of Alberta.

§ Present address: Center for Neurologic Diseases, Brigham & Women's Hospital, Boston, MA 02113.

|| Protein Engineering Network Centres of Excellence, University of Alberta.

⊥ MRC of Canada Group in Protein Structure and Function, University of Alberta.

Present address: Department of Biochemistry, University of Western Ontario, London, Ontario, Canada N6A 5C1.

▽ University of Western Ontario.

[1] Abbreviations: CoA, coenzyme A; DTNB, 5,5′-dithiobis(2-nitrobenzoic) acid; AHA, acetohydroxamic acid; MMP, methylmercaptopropionate; PCR, polymerase chain reaction; 2ME, 2-mercaptoethanol; PMSF, phenylmethylsulfonyl fluoride; PAGE, polyacrylamide gel electrophoresis; ESI-MS, electrospray ionization mass spectrometry; far-UV CD, far-ultraviolet circular dichroism; GuHCl, guanidine hydrochloride; AEC, active enzyme centrifugation; DTT, dithiothreitol.

10.1021/bi0003184 CCC: $19.00
Published on Web 08/18/2000

A nicked enzyme form, which is fully active, is observed in preparations of eukaryotic succinyl-CoA:3-ketoacid CoA transferase purified in the absence of proteinase inhibitors (*2*, *6*, *8*, *12*). The site of proteolysis occurs in the loop of the proposed helix−turn−helix linker, generating N- and C-terminal fragments of molecular weight 2.8×10^4 and 2.4×10^4, respectively. A "hinge-mutant" of pig heart CoA transferase, in which the N- and C-domains are produced as separate polypeptides, is assembled to the active enzyme form in cells of *Escherichia coli* (*13*). In addition, the individually purified N- and C-domains interact to form active CoA transferase in vitro (*13*). Both the hinge-mutant produced in *E. coli* and the complex formed from the isolated domains in vitro consist of two N-domains and two C-domains. Thus, results from experiments aimed at reconstituting the enzyme from its domains provide additional support for the homodimeric structure of intact CoA transferase.

In contrast to the eukaryotic enzymes, the prokaryotic CoA transferases adopt various quaternary structures. Depending on the arrangement of their subunits, the bacterial enzymes can be conveniently grouped into two families (*14*). First are the "$\alpha_2\beta_2$" heterotetrameric CoA transferases consisting of two different types of polypeptides, designated α and β, whose amino acid sequences align with those of the N- and C-domains of the eukaryotic monomer, respectively (*15*, *16*). Enzymes in this category have been identified in bacteria such as *E. coli* (*17*), *Pseudomonas putida* (*15*), *C. acetobutylicum* (*18*, *19*), and *Acinetobacter calcoaceticus* (*20*, *21*). The second family of prokaryotic CoA transferases are referred to as "nonheterotetrameric", and lack both an $\alpha_2\beta_2$-subunit arrangement and significant amino acid sequence similarity to the eukaryotic CoA transferases. Some enzymes in this family consist of only one type of polypeptide, designated α. Examples include the α_4-homotetramer of *C. aminovalericum* (*22*), the α_2-homodimer of *C. aminobutyricum* (*23*), and the α-monomer of *Oxalobacter formigenes* (*24*). Other enzymes consist of two separate polypeptides but in an $\alpha_4\beta_4$ quaternary structure. Glutaconate-CoA transferase from *Acidaminococcus fermentans* is an especially noteworthy example, as it is the only CoA transferase for which an X-ray structure is currently available (*25*−*27*).

During routine purifications of recombinant pig heart CoA transferase produced in cells of *E. coli*, we observed that in the later stages the enzyme eluted as two separate peaks from a gel filtration column. This suggested, as one possibility, that the eukaryotic CoA transferases can adopt multiple quaternary structures reminiscent of the prokaryotic enzymes. To address this hypothesis, we have isolated and characterized the two forms of pig heart CoA transferase, as described in the following report. The two species, referred to initially as the "small" and "large" conformers, were compared with respect to catalytic efficiency, various physicochemical and spectral properties, and equilibrium unfolding. In addition, studies were carried out to investigate the possible interconversion of the two forms. Specific molecular contacts that account for the assembly of a higher order oligomer of pig heart CoA transferase were identified. Finally, we proved that the large conformer exists in pig heart tissue and is therefore physiologically relevant. The existence of different quaternary structures presents an additional level of complexity which must be considered during studies of the folding and assembly of eukaryotic CoA transferases.

EXPERIMENTAL PROCEDURES

Materials. The restriction endonucleases and T4 DNA ligase were purchased from New England Biolabs, Inc., or as Gibco BRL products from Life Technologies, with no obvious differences. Acrylamide and *Taq* DNA polymerase were also obtained as Gibco BRL products from Life Technologies. The T4 DNA polymerase was obtained from Boehringer Mannheim, while the deoxynucleotide triphosphates were supplied by Pharmacia Biotech. The gel filtration calibration kits and the column matrixes DEAE Sephacel, Sephadex G-50, Sephadex G-200, and Sephacryl S-200 were also purchased from Pharmacia Biotech. The column matrixes Affi-Gel Blue and Bio-Gel A were supplied by Bio-Rad Laboratories, Ltd. The β-hydroxyacyl-CoA dehydrogenase, NADH, and lyophilized trypsin were obtained from Sigma Chemical Co. The substrates acetoacetate, acetoacetyl-CoA, and succinyl-CoA were also supplied by Sigma Chemical Co., while succinate was purchased from Eastman Kodak Co. Purified protein preparations were concentrated using Millipore brand Ultrafree-15 concentrators (MWCO $= 1.0 \times 10^4$) or Centricon Plus-80 concentrators (MWCO $= 3.0 \times 10^4$). Dialyses were carried out using Spectra/Por membranes (MWCO $= 3.5 \times 10^3$ or 1.2×10^4), supplied by Spectrum. Finally, the GuHCl was provided by ICN Biomedicals, Inc.

Site-Directed Mutagenesis. A cDNA encoding the "Δ249−254" mutant of CoA transferase, which lacked amino acid residues 249 to 254[2] in the hydrophilic linker, was synthesized in three steps using standard protocols for the polymerase chain reaction (PCR) and overlap extension (*28*, *29*). The template for the PCR was the expression vector pT7-WT (*13*). A full-length mutant cDNA was synthesized using the internal primers HNGDEL (5′-**TTATCAGTCCGGAAAGAGTCTGGTAAGCTTGGAGAT**-3′) and $HNGDEL_C$ (complementary to HNGDEL), and the external primers NDE and HIND (*13*). The amplified cDNA was subcloned as a 0.55 kb *Bam*HI−*Msc*I fragment into pT7-WT, generating pT7-Δ249−254. The absence of possible mutations due to misincorporation by *Taq* DNA polymerase during the PCR was confirmed by automated sequence determinations using previously described methods (*30*) and an Applied Biosystems (ABI) 373A DNA sequencer.

Gene Expression and Protein Purification. Gene expression in cultures of *E. coli* BL21(DE3) and the subsequent preparation of cell lysates were carried out as described previously (*13*). Wild-type or mutant CoA transferases were purified using established procedures (*13*).

The small and large oligomeric forms of CoA transferase were separated by gel filtration chromatography through Sephacryl S-200. Prior to gel filtration, the enzyme solution was concentrated by precipitation in $(NH_4)_2SO_4$ [final concentration, 50% (w/v)] or by centrifugation [$(2 \times 10^3)g$] using Ultrafree-15 concentrators (MWCO $= 1.0 \times 10^4$) or Centricon Plus-80 concentrators (MWCO $= 3.0 \times 10^4$). The

[2] The numbering is based on the sequence of the mature form of the enzyme as reported by Rochet et al. (*13*). Note: residues 249−254 of the mature protein deleted in the hinge mutant correspond to residues 288−293 of the precursor form of CoA transferase (*8*).

protein was eluted using buffer A [0.01 M potassium phosphate, 0.1 mM EDTA, 10 mM 2-mercaptoethanol (2ME), pH 7.4].

The homogeneity of all protein preparations was confirmed by SDS−PAGE analysis. The protein concentration of solutions of wild-type and mutant CoA transferase was determined from absorbance readings at 278 nm corrected for scatter, using an extinction coefficient value of 0.65 $(mg/mL)^{-1}$ (*13*).

Measurement of Enzyme Activity. For routine estimates, CoA transferase activity was determined spectrophotometrically monitoring the increase in absorbance of acetoacetyl-CoA at 310 nm as described previously (*2*, *13*). The extinction coefficient for acetoacetyl-CoA at 310 nm ($\epsilon_{310\ nm}$) was taken to be $7.8 \times 10^3\ M^{-1}\ cm^{-1}$ under these conditions (*31*). In the present study, the assay solutions used for determining specific enzyme activities contained 0.30 mM succinyl-CoA and 67 mM acetoacetate. All assays were carried out at 25 °C.

Enzyme Kinetics. Measurements for kinetic analyses were performed at 25 °C using previously published procedures (*3*, *5*). The formation of succinyl-CoA from acetoacetyl-CoA (0.05−0.15 mM) and succinate (5.0−40 mM) was monitored by the decrease in $A_{310\ nm}$ in an assay solution of 0.067 M Tris−SO_4 buffer (pH 8.1). The ionic strength of the reaction mixture was adjusted to 1.0 M by the addition of the appropriate amount of Na_2SO_4. An $\epsilon_{310\ nm}$ value of $2.6 \times 10^3\ M^{-1}\ cm^{-1}$ was measured for acetoacetyl-CoA under these conditions, using a standard solution of the substrate at a known concentration (see below). The spectrophotometric traces of the catalyzed reactions were corrected for the background decrease in $A_{310\ nm}$ due to the spontaneous hydrolysis of succinyl-CoA, measured in reaction mixtures just prior to the addition of CoA transferase. The enzyme activity was shown to be proportional to the concentration of enzyme up to 0.080 μg of CoA transferase.

In the reverse direction, unbiased rates of acetoacetyl-CoA formation from succinyl-CoA (0.313−1.25 mM) and acetoacetate (0.020−0.080 mM) could not be measured directly by the increase in $A_{310\ nm}$ due to product inhibition (*3*). Instead, this reaction was coupled to the reduction of acetoacetyl-CoA by β-hydroxyacyl-CoA dehydrogenase, which was monitored by the decrease in $A_{340\ nm}$ reflecting the disappearance of NADH. The assay solution consisted of 0.067 M Tris−SO_4 buffer, 0.15 mM NADH, 0.32 M Na_2SO_4, and 2 μg of β-hydroxyacyl-CoA dehydrogenase, at pH 8.1. The β-hydroxyacyl-CoA dehydrogenase, supplied as a suspension in a saturated $(NH_4)_2SO_4$ solution, was dialyzed against 10 mM Tris-HCl, 1 mM EDTA, and 2 mM 2ME (pH 8.0) prior to use. An $\epsilon_{340\ nm}$ value of $6.22 \times 10^3\ M^{-1}\ cm^{-1}$ was used for NADH under these conditions (*3*, *32*). The initial rates of the catalyzed reaction were corrected for the background decrease in $A_{340\ nm}$ from the spontaneous hydrolysis of acetoacetyl-CoA, observed in reaction mixtures before the addition of CoA transferase. The CoA transferase activity was shown to be linear with respect to the concentration of enzyme up to 0.97 μg of CoA transferase.

The concentration of acetoacetyl-CoA was determined spectrophotometrically, using an $\epsilon_{260\ nm}$ value of $1.6 \times 10^4\ M^{-1}\ cm^{-1}$ for a solution of the substrate prepared in 0.1 M potassium phosphate at pH 7.0 (*33*). To ensure that the observed $A_{260\ nm}$ values were not due to large amounts of free CoA resulting from the hydrolysis of acetoacetyl-CoA, absorbance measurements were carried out using fresh solutions of substrate. The concentration of succinyl-CoA was determined spectrophotometrically using an $\epsilon_{232\ nm}$ value of $4.50 \times 10^3\ M^{-1}\ cm^{-1}$ for a solution of the substrate prepared in 0.10 M Tris-HCl, 10 mM $MgCl_2$, 0.1 M KCl, and 10 mM disodium succinate, at pH 7.5 (*34*). The concentration of NADH in a stock solution prepared with distilled water was calculated using an $\epsilon_{340\ nm}$ value of $6.22 \times 10^3\ M^{-1}\ cm^{-1}$ (*32*).

Kinetic parameters were evaluated and the kinetic mechanism verified using the ordinate-intercept replot method described by Segel (*35*). Standard errors were calculated using accepted formulas for the propagation of error (*36*).

Nondenaturing PAGE Analysis. Nondenaturing polyacrylamide gels consisted of a 3% (w/v) stacking gel (pH 6.8) and a 6% (w/v) resolving gel (pH 8.8). Electrophoresis was carried out at a constant voltage of 200 V, and was terminated between 1.5 and 2 h after the disappearance of the tracking dye from the resolving gel. It was determined empirically that these conditions of electrophoresis were optimal for resolving the bands of the small and large molecules of wild-type CoA transferase.

Mass Spectrometry. Molecular masses were determined by electrospray ionization mass spectrometry (ESI-MS) as described previously (*13*). Protein solutions (1.0 mg/mL, or 19 pmol/μL of the NC monomer) were desalted by dialysis against 10 mM Tris-HCl, pH 8.0. Predicted molecular masses were average masses calculated using the program MacProMass.

Circular Dichroism and Fluorescence Studies. Far-UV circular dichroism (CD) and fluorescence measurements were carried out at 25 °C using a Jasco J-720 spectropolarimeter (Jasco Inc., Easton, MD) and a Perkin-Elmer MPF-44B spectrofluorometer, respectively, as described in a previous study (*13*). Prior to these measurements, each protein sample was dialyzed against buffer X (0.2 M potassium phosphate, 0.1 mM EDTA, 10 mM 2ME, pH 7.4). The enzyme solution was then diluted in buffer X to a final concentration of 0.4−0.6 mg/mL (7.7−12 μM NC monomer) for CD or to 0.1−0.2 mg/mL (1.9−3.8 μM NC monomer) for fluorescence.

Equilibrium Unfolding Studies. Equilibrium unfolding transitions were determined from measurements of $[\Theta_{obs,222\ nm}]$, as outlined by Jaenicke and Rudolph (*37*). Stock solutions of enzyme and denaturant were prepared in buffer X (described above). Preliminary studies were carried out to prove that CoA transferase undergoes reversible denaturation using a sample of unfractionated wild-type enzyme. In the "forward" direction, the unfolding transition was determined by mixing a solution of CoA transferase in various ratios with a stock solution of 8 M urea. In the "reverse" direction, the unfolding transition was determined by mixing a solution of CoA transferase, previously treated overnight at 4 °C with 8 M urea, in various ratios with a solution of enzyme that lacked the denaturant. The solutions prepared by both methods contained different amounts of urea at a fixed protein concentration (4.9 μM NC monomer). The mixtures were incubated for 1 h at 22 °C prior to the measurement of $[\Theta_{obs,222\ nm}]$.

The equilibrium unfolding transitions were then determined for the small and large forms of CoA transferase. The proteins (5.1−8.5 μM NC monomer) were denatured for a

minimum of 1 h at 22 °C in solutions containing different concentrations of urea. Measurements of [$\Theta_{obs,222\ nm}$] were carried out as described above.

Calculation of $[\Delta G_u^{H_2O}]_{app}$ *Values*. To facilitate the numerical analyses of thermodynamic parameters, a reversible "two-state" transition between folded dimers and unfolded monomers was assumed for the small and large forms of CoA transferase and the small form of Δ249−254 (*38*−*40*). Values of the apparent free energy of unfolding in the absence of denaturant ($[\Delta G_u^{H_2O}]_{app}$) were estimated by fitting the data to the following equations (*41*, *42*):

$$y = f_u(y_u + ds[den]) + (1 - f_u)(y_n + ns[den])$$

$$f_u = \{-K_{d,app} + ([K_{d,app}]^2 + 8P_tK_{d,app})^{0.5}\}/4P_t$$

$$K_{d,app} = \exp\{(-[\Delta G_u^{H_2O}]_{app} + m[den])/RT\}$$

where y is the observed ellipticity at 222 nm ([$\Theta_{obs,222\ nm}$]) at a given concentration of denaturant (den); y_n and y_u are the extrapolated ordinate-intercept values of $[\Theta]_{obs}$ for the native and unfolded protein, respectively; ns and ds are the slopes of the baselines for the native and denatured protein, respectively; f_u is the molar fraction of unfolded protein; $K_{d,app}$ is the apparent equilibrium dissociation constant; P_t is the total concentration of monomeric protein in moles per liter; R is the universal gas constant [8.31 J/(mol·K)]; T is the absolute temperature (K); and m is a constant proportional to the increase in the solvent-accessible surface area of the protein upon denaturation (*40*, *43*, *44*). The data were fit to the appropriate equations using the program TableCurve 2D (Jandel Scientific, San Rafael, CA), with values of the square of the correlation coefficient (r^2) generally exceeding 0.98.

Conventional Sedimentation Velocity Analyses. Prior to centrifugation, solutions of the small and large conformers were dialyzed against 50 mM potassium phosphate, 0.15 M KCl, and 1 mM EDTA, at pH 7.4. Sedimentation velocity data were initially obtained using a Beckman Model E analytical ultracentrifuge equipped with schlieren optics. The loading protein concentration was 2.00 mg/mL. Ultracentrifugation was carried out at 5.2×10^4 rpm and 20 °C for a period of 3 h, during which a minimum of 10 schlieren photographs were taken. Subsequent sedimentation velocity measurements were carried out using a Beckman XL-I analytical ultracentrifuge equipped with absorbance optics. The loading protein concentrations were 0.24 and 0.47 mg/mL. Ultracentrifugation was carried out at 5.0×10^4 rpm and 20 °C for a period of 3 h, during which a minimum of 20 absorbance scans were recorded. Data obtained using the Model E ultracentrifuge were analyzed by measuring the radial position of the maximal ordinate of the peak on each schlieren photograph with a Nikon Model 6 microcomparator. Data obtained using the XL-I ultracentrifuge were analyzed by the second moment method (*45*). Values for the observed sedimentation coefficient (s_{obs}) were calculated from the slope terms of plots of ln(r) versus t, where r is the radial position measured from the center of the rotor and t is the time in seconds. Values for $s_{20,w}$ were determined by correcting s_{obs} values to standard solvent and temperature (i.e., water at 20 °C), using the program Sednterp (*46*). The partial specific volume (used as well in the sedimentation equilibrium analyses) was estimated based on the amino acid composition of wild-type CoA transferase (*47*). Values for the intrinsic sedimentation coefficient ($s^0_{20,w}$) and the concentration-dependence coefficient (k_s) were determined by plotting $s_{20,w}$ versus the protein concentration and extrapolating the best-fit line through the points to infinite dilution, using the program TableCurve2D.

Active Enzyme Centrifugation. Active enzyme centrifugation (AEC) was carried out following methodology described previously (*48*, *49*), using a Beckman XL-I analytical ultracentrifuge equipped with absorbance optics. CoA transferase activity was followed by monitoring the formation of acetoacetyl-CoA spectrophotometrically at 310 nm. From preliminary spectrophotometric measurements, we determined the amount of enzyme required to produce a change in $A_{310\ nm}$ of approximately 0.5 in the AEC substrate solution (0.10 M Tris-HCl, 15 mM $MgCl_2$, 2.0 mM succinyl-CoA, and 13 mM acetoacetate, pH 9.2). Under these conditions, a maximum of 20% of the initial enzyme activity was lost during the course of the runs due to product inhibition. Prior to centrifugation, solutions of the small and large conformers were dialyzed against 10 mM Tris-HCl and 15 mM $MgCl_2$, at pH 9.2. To form the synthetic band of enzyme, 10 μL of a solution of CoA transferase was layered onto 0.30 mL of the AEC substrate solution in a Vinograd type I, CFE double-sector centerpiece. The loading protein concentrations were 1.00 and 2.88 μg/mL for the small and large conformers, respectively. Ultracentrifugation was carried out at 5.0×10^4 rpm and 20 °C. A minimum of 15 absorbance scans at 310 nm were recorded at 4 min intervals. Values for the observed sedimentation coefficient (s_{obs}) were determined from plots of ln(r) versus t, where r is the radial position of the maxima of difference curves calculated from successive scanner records and t is the mean time of the corresponding scans. Values for $s_{20,w}$ were calculated as described above.

Sedimentation Equilibrium Analyses. Prior to centrifugation, solutions of the small and large conformers were dialyzed against 50 mM potassium phosphate, 0.15 M KCl, and 1 mM EDTA, at pH 7.4. Sedimentation equilibrium data were obtained at 20 °C using a Beckman XL-I analytical ultracentrifuge equipped with absorbance optics. Samples were loaded into six-sector CFE centerpiece cells at loading concentrations of 0.19, 0.38, and 0.69 mg/mL and centrifuged simultaneously. Ultracentrifugation was carried out at speeds of 6.0×10^3, 9.0×10^3, and 1.2×10^4 rpm, and a total of nine data sets were obtained for both the small and large forms of CoA transferase. To ensure that equilibrium had been attained, the runs were continued until there was no significant difference in scans taken 2 h apart.

The combined sedimentation equilibrium data from nine sets were analyzed using a nonlinear least-squares curve-fitting program, NONLIN (*50*). Various models were tested for possible association/dissociation, where the number of species present ranged from 1 (no association/dissociation) to 5. The goodness of fit and, therefore, the appropriateness of the model being tested were determined by examination of the residuals and minimization of the variances.

Determination of Molecular Weights by Gel Filtration Analysis. A mixture of the small and large conformers (final concentration of each, 5 mg/mL) was eluted from a column of Sephadex G-200 using a buffer of 50 mM potassium phosphate, 0.1 M KCl, pH 7.5. The column was calibrated

with respect to molecular weight in two separate runs with the following protein standards (2.0 mL, 5−10 mg/mL): (run 1) chymotrypsinogen A (2.50×10^4), albumin (6.70×10^4), and catalase (2.32×10^5); (run 2) ribonuclease A (1.37×10^4), ovalbumin (4.30×10^4), and aldolase (1.58×10^5). For each standard, the fraction of the stationary gel volume available for diffusion (K_{av}) was calculated using the formula (*51*):

$$K_{av} = (V_e - V_o)/(V_t - V_o)$$

where V_e is the elution volume of the standard, V_o is the column void volume, and V_t is the total bed volume. The elution volume of Blue Dextran 2000 was taken to be the void volume. All elution volumes were calculated based on the "peak" fraction, determined from measurements of protein absorbance ($A_{280\ nm}$). For each protein standard, the log(molecular weight) was plotted against K_{av} to generate a calibration curve, from which the molecular weights of the small and large forms of CoA transferase were estimated.

Kinetics of Interconversion between Oligomeric Forms. Samples of the large conformer of the wild-type enzyme or the Δ249−254 mutant were diluted in a solution containing 50 mM potassium phosphate, pH 7.4, in the absence or presence of KCl (0.1−2 M). The final protein concentration ranged from 5.0 to 10 μg/mL (96 nM to 0.19 μM NC monomer). In certain experiments, the solutions also contained 0.1 mM EDTA and 2 mM 2ME, with no obvious effect on the results. The solution was incubated at temperatures ranging from 4 to 37 °C, and for times ranging from 6 h to 58 days. Aliquots were periodically removed from the solution and analyzed by nondenaturing PAGE using $AgNO_3$ staining to visualize the protein bands. The relative proportions of the large and small conformers were estimated at different times by visual inspection of the silver-stained gels. From these estimates, a limiting value was determined for the first-order rate constant (k_1) for dissociation of the large molecule to the small form. The Gibbs free energy of activation ($\Delta G^{\ddagger}$) for dissociation of the large form was calculated from k_1 using the equation (*35*):

$$\Delta G^{\ddagger} = -2.3RT \log(k_1 h/k_B T)$$

where R is the universal gas constant [8.31 J/(mol·K)], T is the absolute temperature (K), h is Planck's constant (6.62608×10^{-34} J·s), and k_B is the Boltzmann constant (1.38066×10^{-23} J/K).

Refolding Studies in Vitro. The small and large forms of wild-type CoA transferase or the Δ249−254 mutant were denatured in "unfolding" buffer (6.0 M GuHCl, 0.1 M Tris-HCl, 0.050 M KCl, 0.1 mM EDTA, 1 mM DTT, pH 8.0) at 22 °C for a minimum of 5 h. The concentration of protein in unfolding buffer ranged from 0.38 to 0.63 mg/mL (7.2−12 μM NC monomer). The solutions of the unfolded proteins were then diluted 1:50 (v/v) with "refolding" buffer (0.1 M Tris-HCl, 0.050 M KCl, 0.1 mM EDTA, 1 mM DTT, pH 8.0). The samples were incubated for 3 h at 22 °C before being assayed for enzyme activity and analyzed by nondenaturing PAGE.

Proteolysis Experiments. Limited trypsin digestions were carried out at 22 or 37 °C in a buffer of 0.1 M NH_4HCO_3, pH 8.1. Samples of the hinge-mutant and the small and large forms of wild-type CoA transferase (final concentration, 0.74 or 2.0 mg/mL) were treated with trypsin (final concentration, 3.7×10^{-4} or 0.050 mg/mL, respectively) for various times, before terminating the digestion by freezing in liquid nitrogen. Prior to freezing, aliquots of the solutions of nicked CoA transferase were assayed for enzyme activity. Control samples were prepared by omitting the proteinase. Thawed solutions of the proteolytically nicked proteins were analyzed by nondenaturing PAGE and SDS−PAGE in parallel.

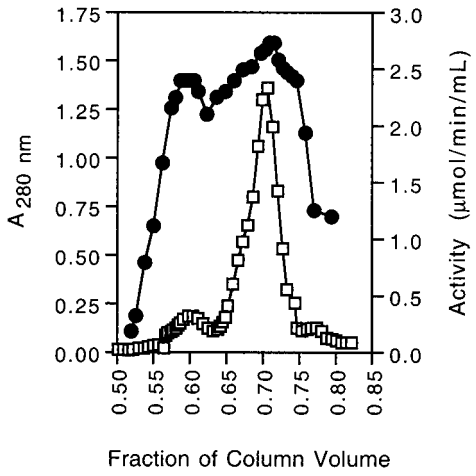

FIGURE 1: Two conformers of wild-type CoA transferase are evident chromatographically. Gel filtration of two different preparations of CoA transferase on a 2.5 × 120 cm column of Bio-Gel A equilibrated and eluted with 5 mM Tris-HCl, 0.1 mM EDTA, 10 mM 2ME, 0.1 mM PMSF, 1 mM benzamidine (pH 8.0). The two elution profiles were determined by assaying aliquots of eluted fractions spectrophotometrically. They have been superimposed based on the fraction of column volume: (□) the elution profile ($A_{280\ nm}$) of purified wild-type enzyme prepared as described under Experimental Procedures; (●) the elution profile (CoA transferase activity) of protein partially purified from pig heart tissue (up to the procedures that use high KCl concentrations) using the method reported by Lin and Bridger (*8*).

RESULTS AND DISCUSSION

Small and Large Forms of Wild-Type CoA Transferase. Preparations of the enzyme that were purified by ion-exchange chromatography consistently eluted as two distinct peaks from a column of Sephacryl S-200, based on measurements of protein absorbance ($A_{280\ nm}$) and CoA transferase activity (cf. Figure 1). From the total absorbance or enzyme activity associated with each peak, it was estimated that the large and small forms accounted, respectively, for 10% and 90% (by mass) of the total protein eluted from the column of Sephacryl S-200.

Using Western blot analysis, we demonstrated that both forms were present in the lysates from cells of *E. coli* that express the cDNA encoding CoA transferase. Thus, the separation of CoA transferase into two molecular species was not an artifact of the preparatory protocols. That pig heart CoA transferase can adopt two quaternary structures may be physiologically relevant (see below) and is reminiscent of the different quaternary structures of CoA transferase observed in prokaryotes.

Sedimentation Velocity Studies. The sedimentation properties of the two forms of CoA transferase were investigated by conventional sedimentation velocity and active enzyme centrifugation (AEC) experiments. The $s^0_{20,w}$ values esti-

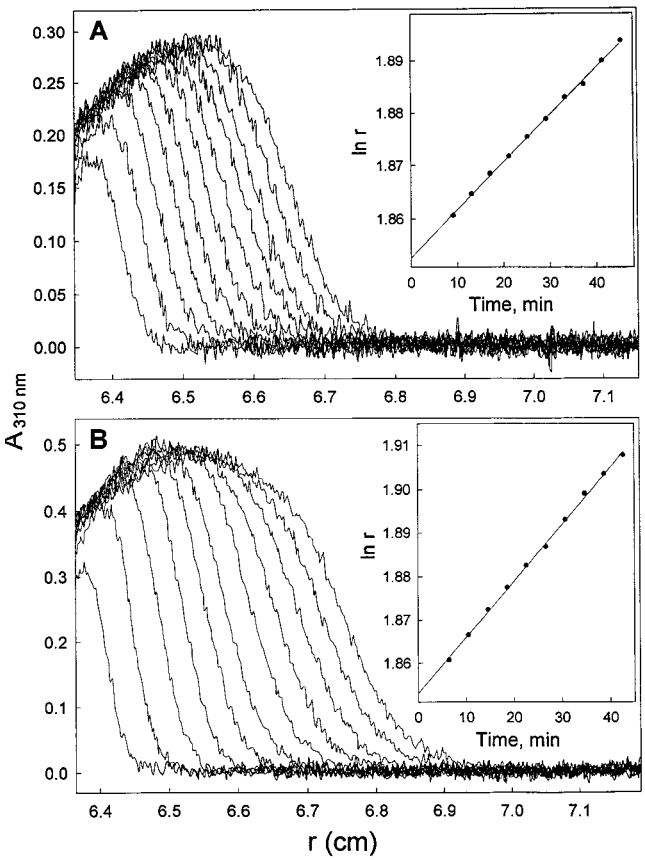

FIGURE 2: Active enzyme centrifugation. Measurements of sedimentation velocity were carried out for the small (A) and large (B) conformers of CoA transferase by monitoring the formation of acetoacetyl-CoA spectrophotometrically at 310 nm. The loading concentrations were 1.0 and 2.9 μg/mL for the small and large forms, respectively. Shown in the main portion of each panel are superimposed tracings from scans taken successively at 4 min intervals. The insets show plots of the logarithm of the radial position (r) of the maxima of difference curves calculated from successive scanner records versus the mean time of the corresponding scans. (See Experimental Procedures for specific details.)

mated for the small and large forms were 5.66 ± 0.07 and 7.90 ± 0.09 S, repectively. This value for the small form agrees well with $s_{20,w}$ values reported for the single molecular species observed in early preparations of CoA transferase (*3*, *6*). Moreover, estimates of the concentration dependence coefficient (k_s) calculated from the slopes were 13 and 11 mL/g, respectively, consistent with nonassociating, globular proteins (*52*).

The apparent sedimentation coefficients determined by AEC at relatively low loading concentrations (Figure 2) were 5.73 and 8.34 S for the small and large species, respectively. These values of $s_{20,w}$, though very similar to the corresponding values determined by conventional sedimentation velocity, were slightly greater, most likely due to the progressive inhibition of the initial enzyme activity by the product acetoacetyl-CoA (*48*, *49*). Nevertheless, it was concluded that the large form of CoA transferase behaves as a discrete, enzymatically active species during sedimentation, even at protein concentrations as low as 3.0 μg/mL.

Determination of Molecular Weights. The apparent molecular weights of the small and large conformers determined by sedimentation equilibrium (Figure 3) were (1.01 ± 0.055) × 10^5 and (2.18 ± 0.085) × 10^5, respectively. Similar results were obtained by gel filtration chromatography (not shown). The molecular weight of the small form was consistent with values determined previously for homodimeric CoA transferase (*3*−*7*), while the apparent molecular weights of the large form indicated a homotetrameric structure.

For both the small and large forms of CoA transferase, the pooled sedimentation equilibrium data were best fit to a single-species model. The goodness of the fit was apparent from the random scatter in the residual plot and the low magnitude of the square-root of the variance (Figure 3). Attempts to fit the data to more complicated models produced a much greater value for the square-root of the variance, suggesting that the small and large conformers did not dissociate or aggregate appreciably under the conditions of sedimentation equilibrium.

Shared Catalytic and Structural Properties of the Two Oligomeric Forms. The homodimeric and homotetrameric enzymes both catalyzed the transfer of CoA via a ping-pong kinetic mechanism, with similar values for k_{cat} and K_M. In addition, the molecular masses of the two conformers, as determined by ESI-MS analyses, were equal within experimental error, indicating that the formation of the homotetramer was not due to a posttranslational modification. The homodimer and homotetramer were also indistinguishable with respect to far-UV CD and intrinsic tryptophan fluorescence (results not shown). Therefore, the two oligomers of CoA transferase have similar secondary structures, and tryptophan residues are not implicated in the intermolecular contacts that stabilize the tetramer.

The equilibrium unfolding of the homodimer and homotetramer in solutions containing different amounts of urea produced superimposable denaturation profiles (results not shown). The results indicated that both oligomers undergo a common equilibrium unfolding transition. Presumably this transition corresponds to the dissociation of nativelike homodimer to unfolded monomer, which suggests in turn that the large molecule dissociates to the small species at a relatively low concentration of denaturant. The values of $[\Delta G_u^{H_2O}]_{app}$ and m, calculated assuming a reversible two-state transition, were similar for the small and large conformers (Table 1). Thus, the subunits of both oligomeric forms have similar conformational stabilities and undergo a similar increase in solvent-accessible surface area upon unfolding (*40*, *43*, *44*). In control experiments, we verified that the unfolding of unfractionated, wild-type CoA transferase is reversible (see Experimental Procedures), with values of $[\Delta G_u^{H_2O}]_{app}$ and m similar to those calculated for the homodimer and homotetramer (Table 1). From the results, we concluded that the subunits of both oligomeric species adopt a common protein fold.

Interconversion of the Homodimer and Homotetramer. If the homotetramer and the homodimer were able to interconvert, then the amount of each species in the unfractionated mixture should vary with the total concentration of enzyme subunits. For example, a significant proportion of the homotetramer should convert to the homodimer in sufficiently dilute protein solutions, according to Le Châtelier's principle. Interconversion between the two oligomeric forms of CoA transferase was conveniently monitored by nondenaturing PAGE. A preparation of the large enzyme form was diluted to a final concentration of 5.0 μg/mL (or 96 nM NC

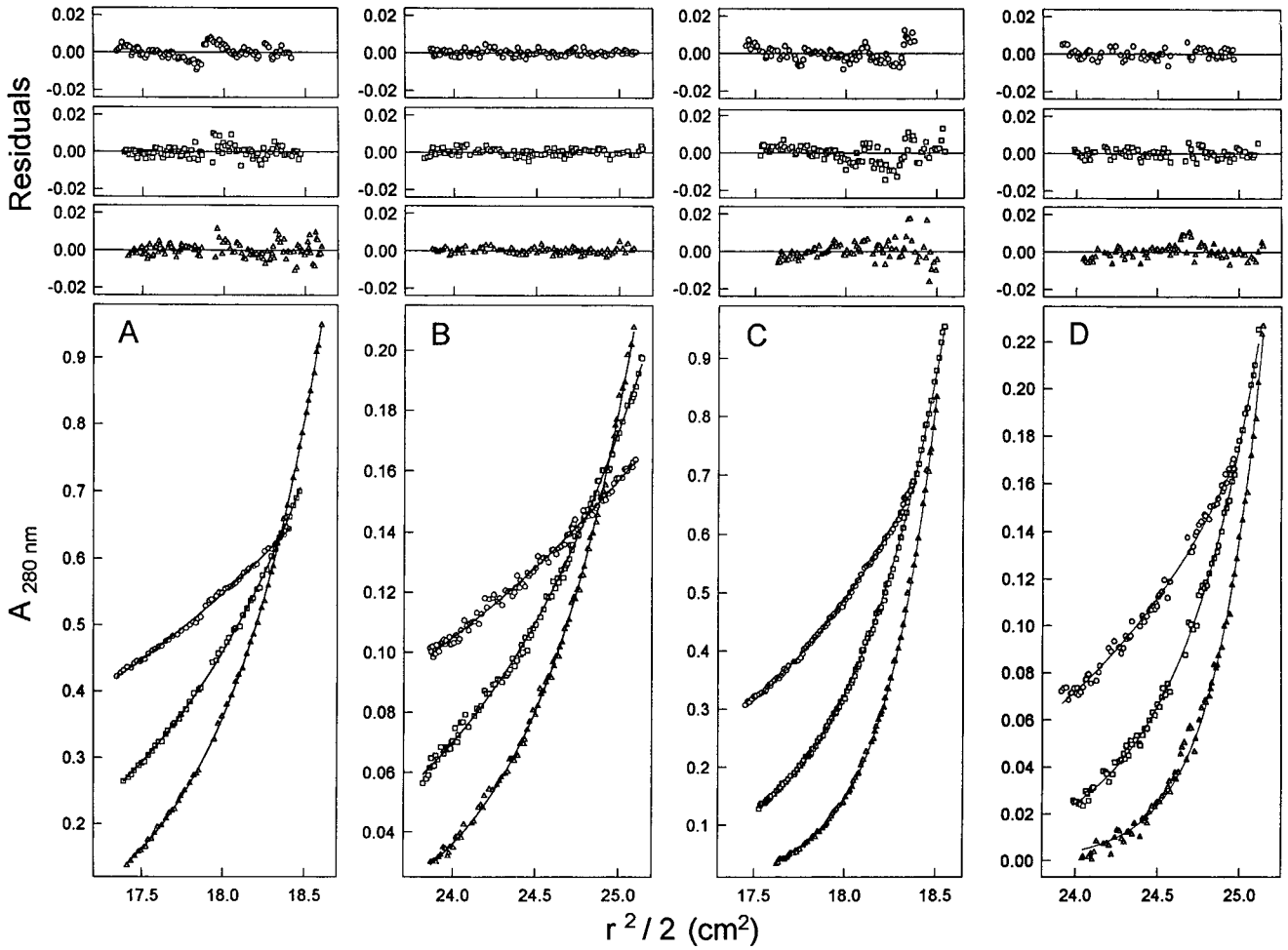

FIGURE 3: Determination of the molecular weights of the two components of wild-type CoA transferase by sedimentation equilibrium. Equilibrium distribution data are shown for the small form (A and B) and the large form (C and D). The ultracentrifugation was carried out at 6.0×10^3 rpm (○), 9.0×10^3 rpm (□), and 1.2×10^4 rpm (△), and the samples were loaded at 0.69 mg/mL (A and C) or 0.19 mg/mL (B and D). Runs for which samples were loaded at 0.38 mg/mL are not shown. The curves represent the best fit to a single-species model, determined from a global analysis of all nine data sets by the program NONLIN. Residuals corresponding to each data set are plotted in the three uppermost panels using the same symbols as in the lower panels. The apparent weight-average molecular weights calculated for the small and large forms were $(1.01 \pm 0.055) \times 10^5$ and $(2.18 \pm 0.085) \times 10^5$, respectively. The square-roots of the variances due to fitting were 3.99×10^{-3} and 7.51×10^{-3} for the small and large components, respectively.

Table 1: Equilibrium Unfolding Parameters for CoA Transferase Denatured with Urea

protein	P_t (μM)	$[\Delta G_u^{H_2O}]_{app}$[a] (kcal/mol)	m[a] (kcal mol^{-1} M^{-1})	$[\text{urea}]_{1/2}$[b] (M)
wild-type CoA transferase				
forward[c]	4.9	13.7 ± 2.0	2.1 ± 0.6	3.1 ± 1.0
reverse[c]	4.9	13.6 ± 1.6	2.0 ± 0.5	3.3 ± 0.9
small molecule	8.5	13.8 ± 0.1	3.5 ± 0.03	2.0 ± 0.02
large molecule	5.1	14.6 ± 0.6	2.8 ± 0.2	2.6 ± 0.2

[a] The error is the standard error due to fitting of the curve, which does not account for systematic errors in the concentration of protein or denaturant. Based on multiple analyses of the reversible denaturation of unfractionated CoA transferase, the true experimental error is in the range of 5−10%. [b] Calculated from: $[\text{urea}]_{1/2} = \{(RT \ln P_t) + [\Delta G_u^{H_2O}]_{app}\}/m$ (*67*). The standard error was determined using accepted formulas for the propagation of error (*36*). [c] "Forward" and "reverse" refer to the method used to determine the equilibrium unfolding transition (see Experimental Procedures).

monomer) with phosphate buffer, and incubated at 4 °C for 2−10 days. Analysis of the diluted samples by nondenaturing PAGE indicated that the large molecule did not dissociate to yield appreciable amounts of homodimer at 4 °C for 58 days, at 22 °C for 48 h, at 30 °C for 24 h, or at 37 °C for 6 h (results not shown). Thus, even during prolonged storage at relatively low protein concentrations, the homotetramer did not dissociate to the homodimer at an appreciable rate.

Next, we considered that the distribution of CoA transferase between the two oligomeric forms might be influenced by the presence of KCl during the purification protocol. If this were true, then the purified large conformer should convert to the small molecule in dilute protein solutions containing salt. A preparation of homotetrameric CoA transferase was diluted to a final concentration of 10 μg/mL (1.9×10^2 nM NC monomer) with phosphate buffer and 1.0 M KCl, and incubated at 22 °C for 6 h to 10 days. Analysis of the diluted samples by nondenaturing PAGE indicated that the large molecule dissociated slowly to the homodimer under these conditions (Figure 4A). It was estimated that approximately 75% of the initial homotetramer was dissociated after 10 days at 22 °C. Next, samples of the large conformer were diluted in solutions containing 0−2.0 M KCl and incubated at 22 °C for 2 days. Analysis of the diluted samples by nondenaturing PAGE indicated that the large molecule dissociated to the small conformer in solutions

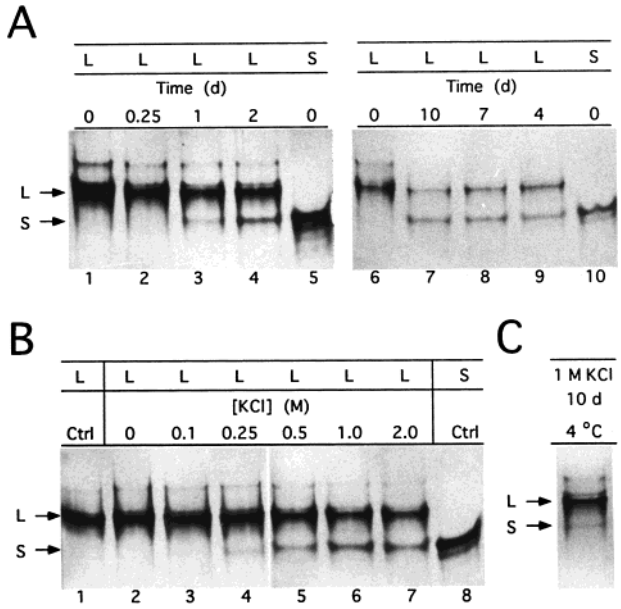

FIGURE 4: Dissociation of homotetrameric CoA transferase in the presence of KCl. Samples of the small (S) and large (L) enzymes (10 μg/mL, or 1.9×10^2 nM NC monomer) were incubated in solutions of 50 mM potassium phosphate, 10 mM 2ME, 0.1 mM EDTA (pH 7.4) with or without KCl for the indicated times prior to analysis by nondenaturing PAGE. (A) Incubations at 22 °C in solutions containing 1.0 M KCl. (B) Incubations at 22 °C for 2 days in solutions containing various final concentrations of KCl from 0 to 2.0 M. (C) Incubation of the large form at 4 °C for 10 days in a solution containing 1.0 M KCl. Bands representing the homotetramer (L) and the homodimer (S) are indicated by appropriately labeled arrows. Each lane was loaded with 1 μg of protein, and the gels were analyzed by staining with $AgNO_3$.

containing a minimum of 0.25 M KCl, and that maximal dissociation occurred in the presence of 1.0 M KCl (Figure 4B). This is consistent with our previous observation that the large conformer did not dissociate to the small species during sedimentation in a solution containing 0.15 M KCl. At 4 °C, the rate of conversion of the homotetramer in solutions containing 1.0 M KCl was substantially lower compared to that at 22 °C. For example, approximately 10% of the initial population of homotetramer dissociated to the homodimer after 10 days at 4 °C, compared with 75% after 10 days at 22 °C (Figure 4C).

Recently, the quaternary structure of the avian sarcoma virus integrase was also shown to be modulated by ionic strength. In this case, dimer formation is favored but tetramer formation is disfavored by increasing salt concentrations in the range of 100−500 mM (*53*). The authors concluded that the dimer and tetramer interfaces of the viral enzyme are characterized by repulsive and attractive Coulombic forces, respectively. Similarly, our results suggest that the CoA transferase homotetramer is stabilized by favorable electrostatic contacts between the two homodimers.

Finally, we predicted that the distribution of CoA transferase between the homodimer and the homotetramer depends on the total protein concentration under denaturing conditions. If this were true, then a proportion of the large conformer unfolded in the presence of denaturant should refold to the small dimeric form upon dilution to a sufficiently low protein concentration. The homodimer and homotetramer were denatured and refolded as described under Experimental Procedures. Nondenaturing PAGE analysis revealed that only the homodimer was present in solutions of the refolded large and small molecules (Figure 5). Similar results were reported for LDH from *Thermotoga maritima* (*54*). Under benign conditions, tetrameric and octameric forms of the enzyme resist interconversion. However, after denaturation of either conformer in GuHCl, the proportion of large and small molecules recovered during refolding is dependent on the protein concentration and the temperature.

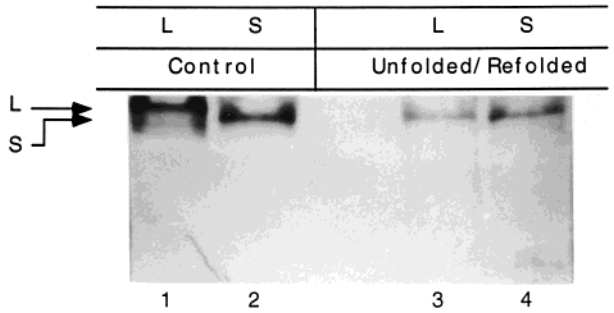

FIGURE 5: Unfolding and refolding of oligomeric forms of CoA transferase. Samples of the small (S) and large (L) enzymes were diluted in "refolding" buffer and analyzed by nondenaturing PAGE. Lanes 1 and 2, control samples diluted without prior denaturation; lanes 3 and 4, samples diluted to a final concentration of 12 μg/mL (or 0.23 μM NC monomer) after unfolding in 6.0 M GuHCl. Bands representing the homotetramer (L) and the homodimer (S) are indicated by appropriately labeled arrows. Each lane was loaded with 1.7 μg of protein, and the gels were analyzed by staining with $AgNO_3$.

From all of these observations, it was inferred that a substantial kinetic barrier separates the two multimeric states of CoA transferase under benign conditions. A limiting value of $\Delta G^{\ddagger} \geq 108$ kJ/mol was estimated for the dissociation of the large molecule to the small oligomeric form at 22 or 30 °C in the absence of salt, assuming that a conversion of at least 10% of the initial homotetramer was detectable by nondenaturing PAGE analysis. A value of $\Delta G^{\ddagger} = 105$ kJ/mol was estimated for the dissociation of the large molecule to the small conformer in the presence of 1.0 M KCl. These values are similar to the $\Delta G^{\ddagger}$ of 112 kJ/mol determined for a slow conformational change in the folding of α-lytic protease (*55*), and for the dissociation of domain-swapped dimers to the corresponding monomers (*56*, *57*). Presumably, the salt causes a lowering of the energy barrier between the homotetramer and the homodimer by disrupting electrostatic interactions and/or by facilitating a conformational rearrangement. In the absence of a kinetic barrier—for example, after unfolding in solutions containing denaturant—the distribution of CoA transferase between the small and large oligomeric forms most likely depends on protein concentration, with low protein concentrations favoring the homodimer.

CoA transferase belongs to a class of proteins that can adopt alternative oligomeric states separated by large kinetic barriers. Other examples include LDH from *Thermotoga maritima* (*54*) and the amyloidogenic protein transthyretin (*58*). The results emphasize that thermodynamics *and* kinetics both play a role in determining the predominant quaternary structure of a protein.

Role of the Hinge Region in the Formation of the Homotetramer. Since the large conformer dissociates slowly in dilute solutions containing salt, we inferred that the homotetramer may be stabilized by contacts between charged

residues. We considered that the hinge region joining the N- and C-domains of CoA transferase may participate in electrostatic interactions that are essential for the stability of the homotetramer, since the linker segment contains a large number of polar residues, most likely organized in an amphipathic helix−turn−helix motif (*8*, *14*, *59*−*61*). Moreover, loop regions have been shown to be critical for the assembly of other oligomeric proteins, including valine dehydrogenase (*62*), plant acetohydroxy acid isomeroreductase (*63*), and yeast thymidylate synthase (*64*).

From previous studies, it was suggested that the hydrophilic linker is relatively exposed to the aqueous solvent and therefore susceptible to the action of proteinases (*2*, *6*, *8*, *12*). We predicted that under suitably mild conditions of proteolysis, the hinge region might be specifically digested while more compact domains remain uncleaved. The controlled digestion of the hinge region could then be a useful approach to determine whether the hydrophilic linker is necessary to stabilize the homotetramer. If so, then the large conformer should be converted directly to the $(NC)_2$-dimer upon proteolysis, without the accumulation of nicked, intermediate forms consisting of four of each domain.

Of the 46 residues that putatively make up the linker, 14 are either Arg or Lys. Accordingly, samples of pure homotetramer, homodimer, and hinge-mutant were treated with trypsin (1/40, w/w) at 37 °C for times ranging from 0 to 60 min as described under Experimental Procedures. After 15 min, both forms of CoA transferase were converted to a common molecular species that migrated more rapidly than the untreated hinge-mutant through a nondenaturing polyacrylamide gel (Figure 6A). It was confirmed by SDS−PAGE that these "clipped" species consisted of two polypeptide fragments with apparent molecular weights of 2.7×10^4 and 2.4×10^4, which corresponded well to the N- and C-domains, respectively, minus the entire linker sequence. Importantly, a complex of intermediate molecular weight, greater than that of the intact hinge-mutant but less than that of the intact homotetramer, was not detected by nondenaturing PAGE analysis of the nicked homotetramer.

The tryptic digestion of the small and large conformers was more extensive than the nicking reported for the CoA transferase of sheep kidney (*6*) or of pig heart (*8*, *12*) isolated in the absence of proteinase inhibitors. As can be seen in Figure 6A, the hinge-mutant itself was degraded to a smaller, partially active enzyme species when treated with trypsin as described above. When the experiment was repeated using milder conditions [1/2000 (w/w) protein/trypsin, at 22 °C], approximately 85% of the initial CoA transferase activity was retained after digestion for 20 min. The results of this second experiment (not shown) suggested that the proteolytic digestion was less extensive and most likely limited to the hydrophilic linker region, generating the enzymatically active nicked form of CoA transferase (*2*, *6*, *8*, *12*). Even under these milder conditions, the homotetramer was converted directly to the $(NC)_2$-dimer, without the accumulation of nicked forms of intermediate molecular weight.

Under all conditions tested, we were unable to limit the digestion to a single cleavage, perhaps because the initial nicking leads to an unfolding of the helical hinge region and thus to an even greater proteolytic sensitivity. Therefore, we are unable to conclude whether a single cleavage of the hydrophilic linker is sufficient to destabilize the homotetramer. Nevertheless, it is clear that the removal of a short segment from the hinge region disrupts the quaternary structure of the large conformer. Consistent with these results, the purified hinge-mutant, analyzed by gel filtration chromatography, eluted as a single, homogeneous species from a column of Sephacryl S-200 (Figure 6B), and did not display

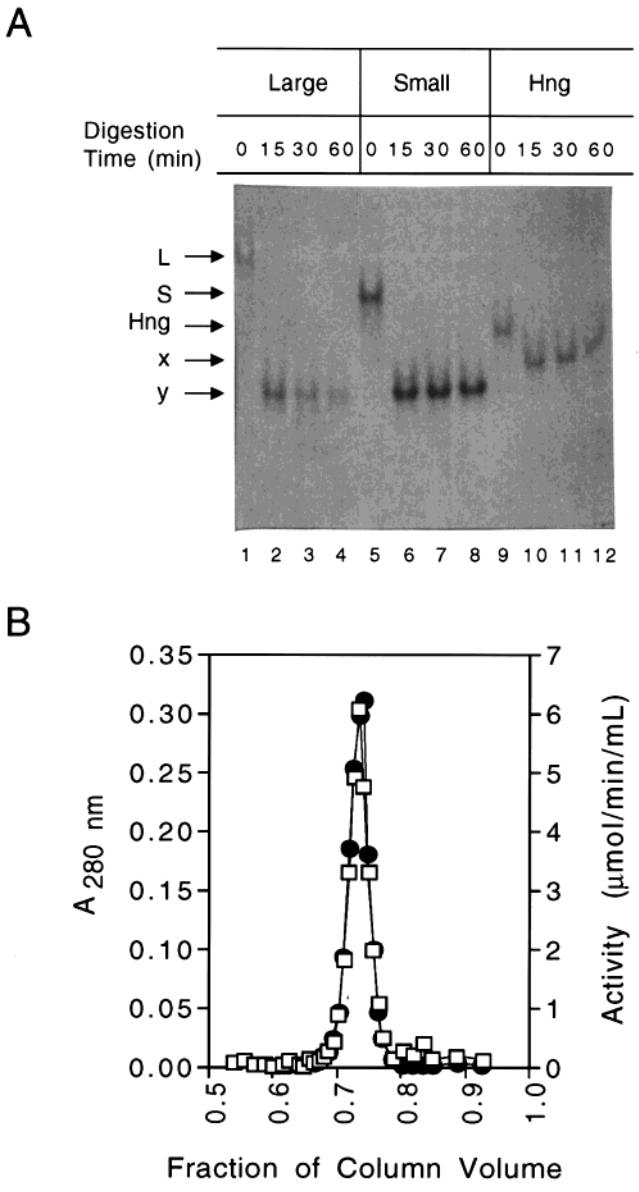

FIGURE 6: Role of the hinge region in stabilizing the homotetramer. (A) Effect of limited tryptic digestion on the stability of homotetrameric CoA transferase. Samples of the large conformer (lanes 1−4), the small conformer (lanes 5−8), and the hinge-mutant (Hng) (lanes 9−12) were treated with trypsin (1/40, w/w) at 37 °C for the indicated times, prior to analysis by nondenaturing PAGE. Bands representing the homotetramer (L), homodimer (S), and hinge-mutant (Hng) are indicated by appropriately labeled arrows. Bands representing low molecular weight species formed by mild proteolysis of the hinge-mutant and the wild-type conformers are also indicated (x and y, respectively). Each lane was loaded with 9 μg of protein, and the gels were analyzed by staining with Coomassie Blue. (B) Analysis of the hinge-mutant by gel filtration chromatography. A sample of enzyme (16 mg/mL, or 3.1×10^2 μM of each domain) eluted as a single peak from a column of Sephacryl S-200 (see Experimental Procedures for details). Aliquots of fractions eluted from the column were assayed spectrophotometrically for protein concentration (□) and CoA transferase activity (●).

a minor peak characteristic of the gel filtration elution profile observed for the wild-type enzyme (Figure 1). Thus, it was concluded that the intact hydrophilic linker is essential for the assembly of the large form of CoA transferase.

The slow rate of dissociation of the homotetramer to the homodimer (see above) suggests that this process occurs via a high-energy intermediate—perhaps a partially unfolded conformer. Speculating further, a structural change involving the hinge region may enable the formation of the high-energy species. Conformational changes involving hinge-loop regions are also thought to facilitate high-energy transitions associated with domain swapping (*56*, *57*).

The Δ249−254 Mutant. Since residues 249−254 of the hydrophilic linker are not present and no longer connect the two domains in the hinge-mutant (*13*), these residues may participate directly in contacts that stabilize the large conformer. If this were true, then a mutant of CoA transferase with an intact linker but lacking amino acid residues 249−254 in the hinge region should consist only of the small oligomeric form. Such a mutant (referred to as "Δ249−254") was constructed, isolated, and subsequently analyzed by gel filtration chromatography. The mutant protein eluted as distinct minor and major peaks from a column of Sephacryl S-200, based on measurements of protein absorbance ($A_{280\ nm}$) and CoA transferase activity (Figure 7A). From the total absorbance associated with each peak, it was estimated that the large and small forms accounted, respectively, for 2% and 98% (by mass) of the total protein eluted from the column. Fractions corresponding to each peak were subsequently pooled, and the resulting enzyme samples were analyzed by nondenaturing PAGE (Figure 7B). The small and large forms of Δ249−254 migrated more rapidly through a nondenaturing polyacrylamide gel than the small and large wild-type conformers, respectively. Thus, it was inferred that a sample of Δ249−254 consists of small and large oligomeric forms with corresponding molecular masses slightly less than those of the wild-type homodimer and homotetramer, respectively.

Under standard assay conditions, the specific activities of the small and large forms of Δ249−254 were virtually identical to those of the wild-type homodimer and homotetramer, respectively. The small and large forms of Δ249−254 were also indistinguishable from the wild-type homodimer and homotetramer with respect to far-UV CD and intrinsic tryptophan fluorescence. Thus, the small and large forms of Δ249−254 are similar in conformation to the homodimeric and homotetrameric variants of wild-type CoA transferase.

To determine whether a kinetic barrier separates the small and large forms of Δ249−254, the dissociation of the large mutant conformer in dilute protein solutions was monitored as described previously for the wild-type homotetramer. In the absence of salt or denaturant, the large form of Δ249−254 did not dissociate to yield appreciable amounts of the small conformer at 4 or 22 °C (results not shown). In a solution containing 1 M KCl, the large form of Δ249−254 converted slowly to the small molecule at 22 °C (Figure 8) but very little at 4 °C (results not shown). It was estimated that approximately 25% of the initial large mutant was dissociated after 10 days at 22 °C in the presence of salt. A value of $\Delta G^{\ddagger} = 109$ kJ/mol was estimated for this conversion, compared to the value of $\Delta G^{\ddagger} = 105$ kJ/mol estimated for the dissociation of the wild-type homotetramer. Finally, after denaturation in GuHCl, the large form of Δ249−254 was converted to the small molecule during refolding at low protein concentrations (results not shown). Thus, as with the wild-type enzyme, a substantial kinetic barrier separates the two multimeric states of Δ249−254.

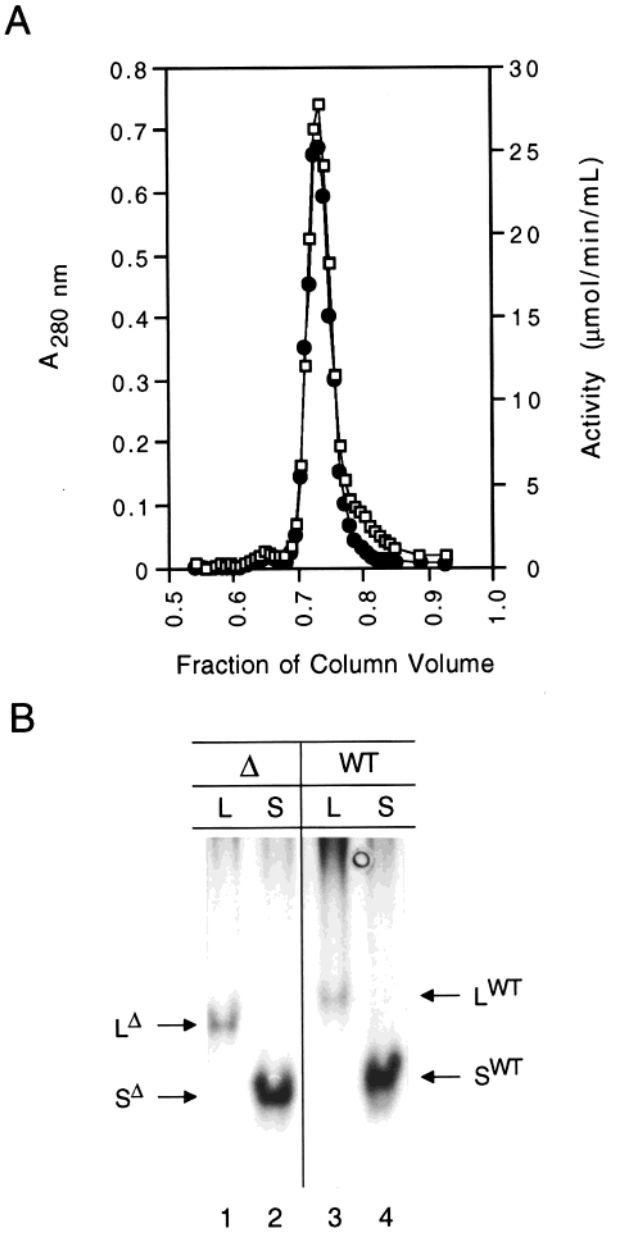

FIGURE 7: Distinct chromatographic and electrophoretic behavior of two forms of the 249−254 deletion-mutant (Δ249−254). (A) Gel filtration. A sample of enzyme (9 mg/mL, or 1.7×10^2 μM NC monomer) was fractionated into two components through a column of Sephacryl S-200. Aliquots of fractions eluted from the column were assayed spectrophotometrically for protein concentration (□) and CoA transferase activity (●). The large and small conformers accounted for 2% and 98% (respectively) of the total protein mass associated with the unfractionated enzyme sample. (B) Nondenaturing PAGE. Lane 1, the large form (L) of Δ249−254; lane 2, the small form (S) of Δ249−254; lane 3, the large form of wild-type CoA transferase; lane 4, the small form of wild-type CoA transferase. Bands representing the large and small forms of the wild-type enzyme (L^{WT} and S^{WT}, respectively), and the large and small forms of Δ249−254 (L^{Δ} and S^{Δ}, respectively) are indicated by appropriately labeled arrows. Each lane was loaded with 15 μg of protein, and the gel was analyzed by Coomassie Blue staining.

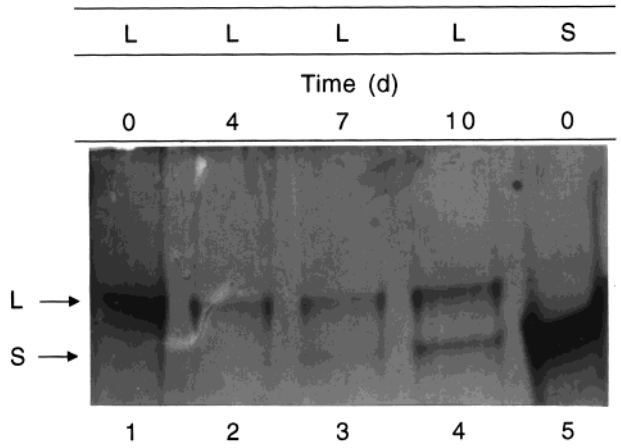

FIGURE 8: Dissociation of the large form of Δ249−254 in the presence of KCl. Samples of the small (S) and large (L) conformers (10 μg/mL, or 1.9×10^2 nM NC monomer) were incubated in, 1 M KCl, 50 mM potassium phosphate, 10 mM 2ME, 0.1 mM EDTA (pH 7.4) at 22 °C for the indicated times prior to analysis by nondenaturing PAGE. Bands representing the homotetramer (L) and the homodimer (S) are indicated by appropriately labeled arrows. Each lane was loaded with 1.0 μg of protein, and the gels were analyzed by staining with $AgNO_3$.

The ratio of homotetramer to homodimer was much lower for the Δ249−254 mutant than for the wild-type enzyme, suggesting that residues 249−254 play a role in stabilizing the large form of CoA transferase. However, because the Δ249−254 mutant was able to adopt a large oligomeric structure, the deletion of residues 249−254 does not on its own account for the absence of the homotetramer in a sample of the hinge-mutant. Perhaps a specific conformation of the hydrophilic linker is also necessary to stabilize the large wild-type conformer. The essential structure of the hinge region, although partially preserved in Δ249−254, would presumably be completely disrupted in the hinge mutant due to the physical separation of the N- and C-domains.

Biological and Evolutionary Implications of the Homotetramer. Does the large form of CoA transferase exist in vivo? Using Western blot analysis, we have confirmed that both the homodimer and the homotetramer are present in the initial lysates from cells of *E. coli* that express the cDNA encoding CoA transferase (results not shown). More importantly, gel filtration chromatography of protein partially purified from pig heart tissue (prior to the procedures that use high KCl concentrations) demonstrated two peaks of CoA transferase activity eluting at relative column volumes corresponding to those observed with the purified, recombinant wild-type enzyme (Figure 1). Thus, the assembly of two homodimers to form the homotetramer occurs under physiological conditions.

As suggested by the similar size of the peaks in Figure 1, the relative amounts of the two forms are almost equal at this early stage of the purification. Given that the large conformer dissociates to the small form in the presence of salt (Figure 4), the lengthy treatment with high KCl concentrations during the latter stages of the standard protocol may explain why the ratio of homotetramer to homodimer is lower at the end of the purification, and even why the large form has been "missed" in previous preparations of CoA transferase. Hersh and Jencks (*3*) reported in an earlier study that the principal peak of sedimenting material accounted for only 85% of the total purified protein. It is conceivable that the remainder, which presumably was dismissed as aggregated or contaminating material, consisted at least in part of the homotetramer. Therefore, previous studies of the active site of CoA transferase may have been carried out using a mixture of the homodimer and homotetramer. Nevertheless, the conclusions from these earlier works are still valid, since the homodimer and homotetramer are catalytically indistinguishable.

The biological rationale for the existence of two oligomeric forms of CoA transferase is unclear. For example, the results of kinetic analyses clearly indicate that the catalytic properties of the small and large conformer are identical. In addition, the small and large conformers are equally susceptible to denaturation, suggesting that the ability to form the homotetramer is not necessary to stabilize the tertiary structure of the CoA transferase subunit. Perhaps the formation of the homotetramer benefits the cell by decreasing the osmotic pressure in the mitochondria, or by burying hydrophobic surfaces that would otherwise lead to protein aggregation in a crowded intracellular environment (*65*, *66*).

Alternatively, the large conformer may not fulfill an essential biological function. Instead, the formation of the homotetramer may merely be a fortuitous consequence of joining the N- and C-domains with the helical hinge, which in turn may be necessary to facilitate a productive interaction between the N- and C-domains during folding of the CoA transferase monomer (*2*). According to this scenario, the hydrophilic linker (and not the homotetrameric form of CoA transferase, per se) would be subject to favorable selective pressures during evolution.

Finally, the homotetrameric form of pig heart CoA transferase may be structurally equivalent to the glutaconate CoA transferase of *Acidaminococcus fermentans*, which exists as an $\alpha_4\beta_4$-heterooctamer (*25*, *26*). In the prokaryotic enzyme, two $\alpha_2\beta_2$-heterotetramers associate to form the heterooctamer via interactions involving the α-helical C-terminal segments of the α-subunits (*27*). These interactions may correspond to the contacts between the hinge regions of neighboring subunits in the homotetrameric form of pig heart CoA transferase. Glutaconate CoA transferase does not belong to the "$\alpha_2\beta_2$" family of prokaryotic CoA transferases, and therefore lacks significant sequence similarity with the mammalian enzyme (*14*, *27*). Nevertheless, the fact that glutaconate CoA transferase and the pig heart enzyme adopt similar oligomeric structures suggests that primary *and* quaternary structural information must both be considered when assessing evolutionary relationships between the prokaryotic and eukaryotic CoA transferases.

ACKNOWLEDGMENT

We thank Brian Tripet and Lorne Burke for their technical assistance with the mass spectrometry. We are also grateful to Perry d'Obrenan for the oligonucleotide syntheses and the DNA sequencing, and to Roger Bradley for the photography work.

REFERENCES

1. Jenkins, T. M., and Weitzman, P. D. J. (1986) *FEBS Lett. 205*, 215−218.
2. Rochet, J.-C., and Bridger, W. A. (1994) *Protein Sci. 3*, 975−981.

3. Hersh, L. B., and Jencks, W. P. (1967) *J. Biol. Chem. 242*, 3468−3480.
4. Edwards, M. R., Singh, M., and Tubbs, P. K. (1973) *FEBS Lett. 37*, 155−158.
5. White, H., and Jencks, W. P. (1976) *J. Biol. Chem. 251*, 1708−1711.
6. Sharp, J. A., and Edwards, M. R. (1978) *Biochem. J. 173*, 759−765.
7. Russell, J. J., and Patel, M. S. (1982) *J. Neurochem. 38*, 1446−1452.
8. Lin, T., and Bridger, W. A. (1992) *J. Biol. Chem. 267*, 975−978.
9. White, H., Solomon, F., and Jencks, W. P. (1976) *J. Biol. Chem. 251*, 1700−1707.
10. Pickart, C. M., and Jencks, W. P. (1979) *J. Biol. Chem. 254*, 9120−9129.
11. Kindman, L. A., and Jencks, W. P. (1981) *Biochemistry 20*, 5183−5187.
12. Moore, S. A., and Jencks, W. P. (1982) *J. Biol. Chem. 257*, 10893−10907.
13. Rochet, J.-C., Oikawa, K., Hicks, L. D., Kay, C. M., Bridger, W. A., and Wolodko, W. T. (1997) *Biochemistry 36*, 8807−8820.
14. Rochet, J.-C. (1998) Ph.D. Thesis, University of Alberta, Edmonton, Canada.
15. Parales, R. E., and Harwood, C. S. (1992) *J. Bacteriol. 174*, 4657−4666.
16. Kassovska-Bratinova, S., Fukao, T., Song, X.-Q., Duncan, A. M. V., Chen, H. S., Robert, M.-F., Pérez-Cerdá, C., Ugarte, M., Chartrand, C., Vobecky, S., Kondo, N., and Mitchell, G. A. (1996) *Am. J. Hum. Genet. 59*, 519−528.
17. Sramek, S. J., and Frerman, F. E. (1975) *Arch. Biochem. Biophys. 171*, 14−26.
18. Fischer, R. J., Helms, J., and Dürre, P. (1993) *J. Bacteriol. 175*, 6959−6969.
19. Petersen, D. J., Cary, J. W., Vanderleyden, J., and Bennett, G. N. (1993) *Gene 123*, 93−97.
20. Kowalchuk, G. A., Hartnett, G. B., Benson, A., and Houghton, J. E., Ngai, K.-L., and Ornston, L. N. (1994) *Gene 146*, 23−30.
21. Shanley, M. S., Harrison, A., Parales, R. E., Kowalchuk, G., Mitchell, D. J., and Ornston, L. N. (1994) *Gene 138*, 59−65.
22. Eikmanns, U., and Buckel, W. (1990) *Biol. Chem. Hoppe-Seyler 371*, 1077−1082.
23. Scherf, U., and Buckel, W. (1991) *Appl. Environ. Microbiol. 57*, 2699−2702.
24. Baetz, A. L., and Allison, M. J. (1990) *J. Bacteriol. 172*, 3537−3540.
25. Buckel, W., Dorn, U., and Semmler, R. (1981) *Eur. J. Biochem. 118*, 315−321.
26. Mack, M., Bendrat, K., Zelder, O., Eckel, E., Linder, D., and Buckel, W. (1994) *Eur. J. Biochem. 226*, 41−51.
27. Jacob, U., Mack, M., Clausen, T., Huber, R., Buckel, W., and Messerschmidt, A. (1997) *Structure 5*, 415−426.
28. Higuchi, R., Krummel, B., and Saiki, R. K. (1988) *Nucleic Acids Res. 16*, 7351−7367.
29. Ho, S. N., Hunt, H. D., Horton, R. M., Pullen, J. K., and Pease, L. R. (1989) *Gene 77*, 51−59.
30. Sanger, F., Nicklen, S., and Coulson, A. R. (1977) *Proc. Natl. Acad. Sci. U.S.A. 74*, 5463−5467.
31. Howard, J. B., Zieske, L., Clarkson, J., and Rathe, L. (1986) *J. Biol. Chem. 261*, 60−65.
32. Horecker, B. L., and Kornberg, A. (1948) *J. Biol. Chem. 175*, 385−390.
33. Stadtman, E. R. (1957) *Methods Enzymol. 3*, 931−941.
34. Bridger, W. A., Ramaley, R. F., and Boyer, P. D. (1969) *Methods Enzymol. 13*, 70−75.
35. Segel, I. H. (1975) *Enzyme Kinetics*, John Wiley and Sons, Inc., New York.
36. Parratt, L. G. (1961) *Probability and Experimental Errors in Science*, John Wiley and Sons, Inc., New York.
37. Jaenicke, R., and Rudolph, R. (1986) *Methods Enzymol. 131*, 218−250.
38. Pace, C. N. (1975) *Crit. Rev. Biochem. 3*, 1−43.
39. Pace, C. N. (1986) *Methods Enzymol. 131*, 266−280.
40. Shortle, D. (1989) *J. Biol. Chem. 264*, 5315−5318.
41. De Francesco, R., Pastore, A., Vecchio, G., and Cortese, R. (1991) *Biochemistry 30*, 143−147.
42. Milla, M. E., Brown, B. M., and Sauer, R. T. (1993) *Protein Sci. 2*, 2198−2205.
43. Schellman, J. (1978) *Biopolymers 17*, 1305−1322.
44. Myers, J. K., Pace, C. N., and Scholtz, J. M. (1995) *Protein Sci. 4*, 2138−2148.
45. Goldberg, R. J. (1953) *J. Phys. Chem. 57*, 194−202.
46. Sedimentation Interpretation Program, Version 1.01. (1998) Created by David B. Hayes (Magdelan Colledge), Tom Laue (University of New Hampshire), and John Philo (Amgen).
47. Cohn, E. J., and Edsall, J. T. (1943) in *Proteins, Amino Acids, and Peptides* (Cohn, E. J., and Edsall, J. T., Eds.) pp 370−377, Hafner Publishing Company, Inc., New York.
48. Cohen, R., and Mire, M. (1971) *Eur. J. Biochem. 23*, 267−275.
49. Kemper, D. L., and Everse, J. (1973) *Methods Enzymol. 27*, 67−82.
50. Johnson, M. L., Correia, J. J., Yphantis, D. A., and Halvorson, H. R. (1981) *Biophys. J. 36*, 575−588.
51. Andrews, P. (1965) *Biochem. J. 96*, 595−606.
52. Teller, D. C. (1973) *Methods Enzymol. 27*, 346−441.
53. Coleman, J., Eaton, S., Merkel, G., Skalka, A. M., and Laue, T. (1999) *J. Biol. Chem. 274*, 32842−32846.
54. Dams, T., Ostendorp, R., Ott, M., Rutkat, K., and Jaenicke, R. (1996) *Eur. J. Biochem. 240*, 274−279.
55. Baker, D., Sohl, J. L., and Agard, D. A. (1992) *Nature 356*, 263−265.
56. Bennett, M. J., Schlunegger, M. P., and Eisenberg, D. (1995) *Protein Sci. 4*, 2455−2468.
57. Schlunegger, M. P., Bennett, M. J., and Eisenberg, D. (1997) *Adv. Protein Chem. 50*, 61−122.
58. Lai, Z., McCulloch, J., Lashuel, H. A., and Kelly, J. W. (1997) *Biochemistry 36*, 10230−10239.
59. Chou, P. Y., and Fasman, G. D. (1978) *Adv. Enzymol. Relat. Areas Mol. Biol. 47*, 45−148.
60. Levitt, M. (1978) *Biochemistry 17*, 4277−4285.
61. Deléage, G., and Roux, B. (1987) *Protein Eng. 1*, 289−294.
62. Turnbull, A. P., Baker, P. J., and Rice, D. W. (1997) *J. Biol. Chem. 272*, 25105−25111.
63. Wessel, P. M., Biou, V., Douce, R., and Dumas, R. (1998) *Biochemistry 37*, 12753−12760.
64. Munro, E. M., Climie, S., Vandenberg, E., and Storms, R. K. (1999) *Biochim. Biophys. Acta 1430*, 1−13.
65. Eisenstein, E., and Schachman, H. K. (1989) in *Protein Function: a Practical Approach*, IRL Press at Oxford University Press, Oxford.
66. Goodsell, D. S., and Olson, A. J. (1993) *Trends Biochem. Sci. 18*, 65−68.
67. Mok, Y.-K., Prat Gay, G. de, Butler, P. J., and Bycroft, M. (1996) *Protein Sci. 5*, 310−319.

BI0003184